APPLICATION OF GEOPHYSICS FOR GROUNDWATER EVALUATION IN HARDROCK: CASE STUDY: KITUI FAULT ZONE

E. N. Muturi[1], M. O. Korowe[1], J. G. Githiri[1], I. Cezar[2] and S. Jeffrey[3]
[1]Jomo Kenyatta University of Agriculture and Technology, Nairobi, Kenya
[2]The Romanian Society of Geophysicists, Bucharest, Romania
[3]The University of Western Australia
E-mail: essynmuturi@gmail.com

Abstract
The lack of access to potable water in Kitui has resulted to severe droughts causing poverty, famine and high infant mortality rates, which has risen to 9.8% and life expectancy is declining steadily. The fact that the basement system is hard Precambrian rock, ground water tends to be more localized and thus sustainable wells cannot be dug on a trial and error basis. The aim of this project was to evaluate groundwater potential located in the concealed fractured /faulted zones which act as groundwater storage and conduits, using magnetic and geo-electrical geophysical techniques. A terrameter was used to collect resitivity data and subsequently determine the subsurface layer resistivity anomalies using Wenner profiling and resistivity sounding inversion software, IP2WIN. Proton precession magnetometer was used to measure the total magnetic field intensity of the earth and 2D Euler deconvolution software was used to model the disintegrated basement. Magnetic surveys showed distinct magnetic anomalies signifying sudden disruption of the basement rock which occur due to faulting. Resistivity surveys also showed low resistivity anomaly at points of significant magnetic anomaly. This suggests groundwater potential in the inferred fault.

Key words: groundwater elevation, geophysical techniques, magnetic field, sounding inversion software, resistivty

1.0 Introduction

1.1 Background of Study

The five continents around the world have varied challenges; however clean drinking water has lately become a common challenge for all of us. This is mainly due to the change in climate, which has resulted to the unreliable rainfall and the severe droughts which make surface water unreliable. Underground water has thus been explored successfully using different geophysical techniques in different parts of the world to substitute for the limited clean surface water.

Surface geophysical survey as an instrument in groundwater exploration has the basic advantage of saving cost in borehole construction by locating aquifer before embarking upon drilling. According to Hasbrouck and Morgan (2003), the financial investment in a groundwater production well can often approach up to $25,000, depending on the drilling depth. However surface geophysical methods can reduce the risk of off-target drilling and enhance borehole drilling on high potential zones.

Most of the rocks which are non porous can be classified as hard rock. In these dense rocks, groundwater occurs in the weathered or the fractured zones. The nature and extent of weathering, especially in igneous and metamorphic rocks depend mostly on the existence of fracture systems. This is essential for ground water accumulation. From Petangay and Murali (1998) study, hard rock areas are characterized by extreme variations of permeability in vertical and horizontal directions and this leads to highly localized water producing zones and of varying yield tendencies. For this reason, groundwater prospecting in hard rock areas cannot be done in a random manner, hence the need to apply geophysics. Pure groundwater is a rare occurrence in nature and water generally contains a small percentage of some salts, such as sodium chloride and potassium chloride. However, the presence of moisture containing salts in hard rock is limited to very small amounts due to the inherent low primary porosity, usually not exceeding 1% (Petangay and Murali, 1998).

The resistivity of rock formations, according to Keys *et al*., (1971) depends on such internal factors as mineralogical and chemical content, grain size, porosity, texture and structure. Other factors of external origin such as moisture, salinity, temperature also influences resistivity of the formation. Thus, most hard rock systems have highly dense

and well cemented formations and thus are highly resistive. In hard basement rocks, electricity is majorly conducted electrolytically by the interstitial fluid. Therefore Keys concludes that in groundwater evaluation, electric conductivity of a rock defines the amount of fluid contained in the rock, salinity of the fluid, pore interconnection/ fracture.

Magnetic susceptibility is also an important physical property of geological formations which is applied in exploration. Petangay and Murali (1998) defined it as the extent to which a body is magnetized in the presence of an ambient magnetic field. The magnetic response of the rocks is directly proportional to the susceptibility of minerals contained hence susceptibility depends only on the presence, distribution and nature of ferromagnetic mineral. Susceptibility contrasts on disintegrated basement system will be used to map out faulting and fracturing which act as groundwater conduits and whose intersection provides for a high yielding aquifer. Therefore application of the magnetic method will delineate the disintegrated basement structure and its lithology.

Fractures are the primary source to store and allow movement of groundwater in hardrock areas. Sharma and Baranwal (2005) determined that the size and location of the fractures, interconnection of the fractures, and amount of the material that may be clogging the fractures and recharging sources determine how much water one can get out of the hard rock. When fractures become narrower at depth, this amount further decreases. Thus the total amount of water storage in the fractures of hard rock area may be small; hence, groundwater levels and the well's yield can decline dramatically during the dry season. Sharma and Baranwal (2005) therefore concluded that the success in locating a high yielding borehole is greatly dependent on intersecting fractures in the bedrock basement. However, a study by Barker (2001) showed that, when thick weathered rock covers these fractures, it becomes very difficult to find them. He suggested that the most important feature is that where fractures are present, the bedrock is expected to be more strongly weathered to a greater depth than where it is unfractured. This is because the presence of fractures and joints facilitate the downward percolation of water that then causes increased weathering. It is therefore possible to use magnetic to discriminate between weathered rock, which often has weak magnetization, and fresh rock to detect intersecting fractures.

1.2 Study Area

The area of study is Nzwani, Kitui County, in the Eastern part of Kenya. The very old and hard Precambrian basement is dominant in this area of study. This hard rock basement system is mainly comprised of gneisses schists and crystalline limestone rock. Nyamai et al., (2003) indicated a large and extensive fracture zone is centrally placed along the longitudinal axis of the district. This is seen as a single fault on the geological map of Kenya (Figure 1) but is in fact a grouping of parallel trending faults and fractures. The 100km long by 2km wide concealed mutito fault is covered by recent sandy alluvium deposits which makes geologic inference difficult. A geological report by Saggerson, (1957) shows a geological structural map (Figure 2) which infers the concealed Mutito fault zone.

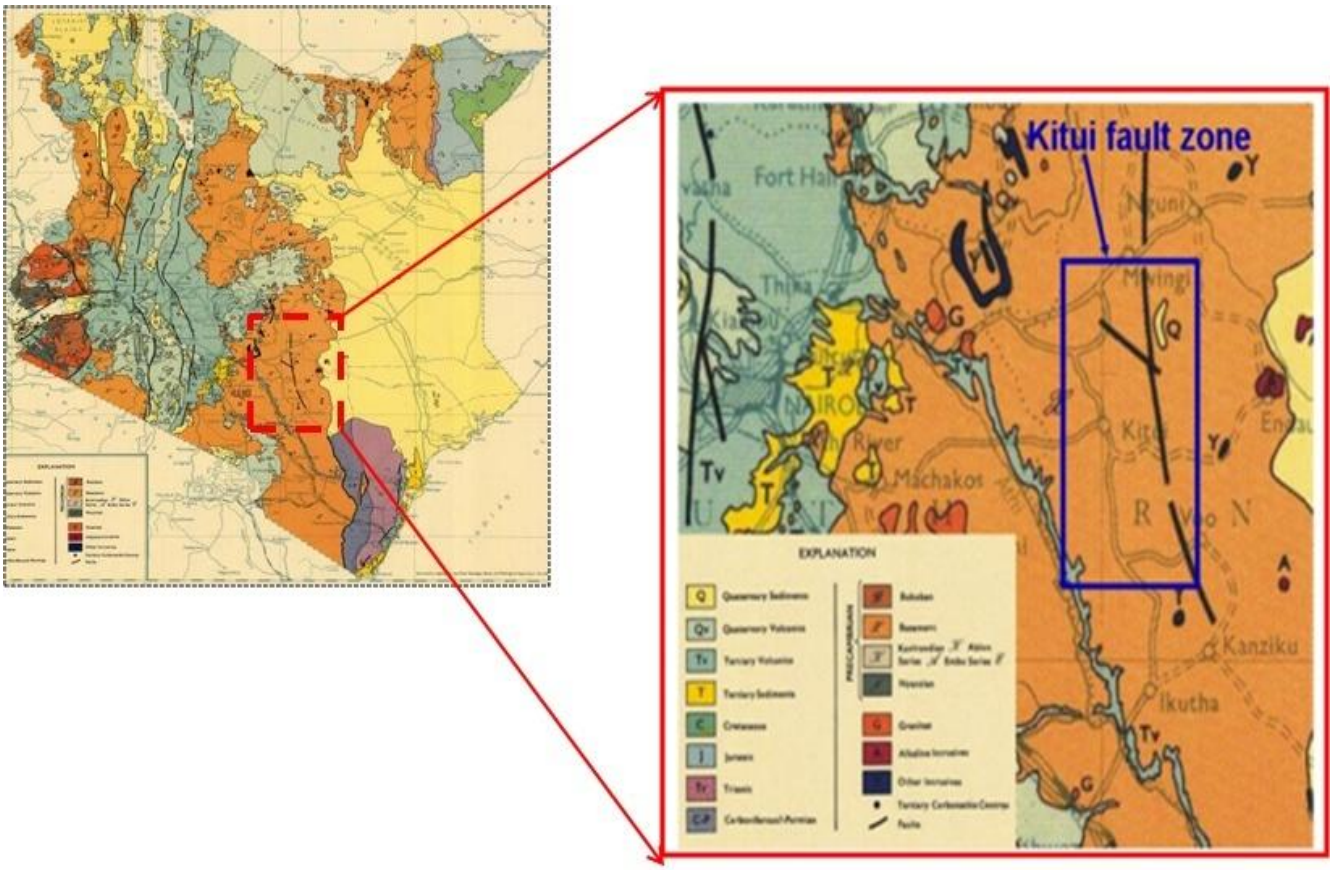

Figure 1: Geological Map of Kenya; (Bottom blue boundary rectangle) Location of Study area, Kitui fault zones (Nyamai et al., 2003)

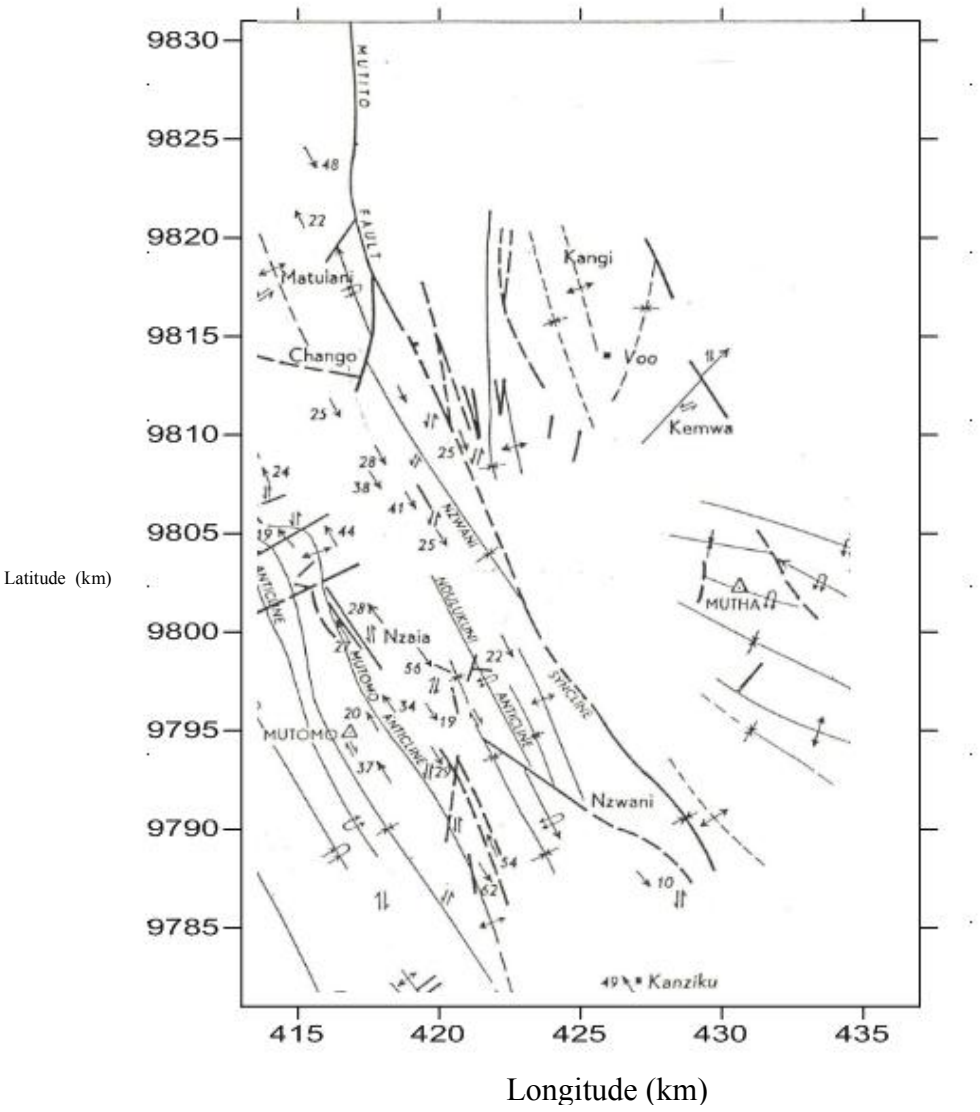

Figure 2: Structural map of the Mutito fault, within the Kitui Fault zone (Saggerson, 1957)

The concealed Mutito fault zone is geologically inferred to be where the dashed line is placed. A syncline also exists (Figure 2) where the stipulated fault is inferred to be. This will provide for a perfect set up for groundwater catchment.

A detailed geologic map of the South Kitui region, Figure 3, shows a complex folded basement with rock outcrops at higher elevations. The presumed extension of the Mutomo Fault is shown as the thick green line through the Mathima Valley, which is also depicted, with dashed line, in the structural map above, Figure 2, and it represents the main target this investigation

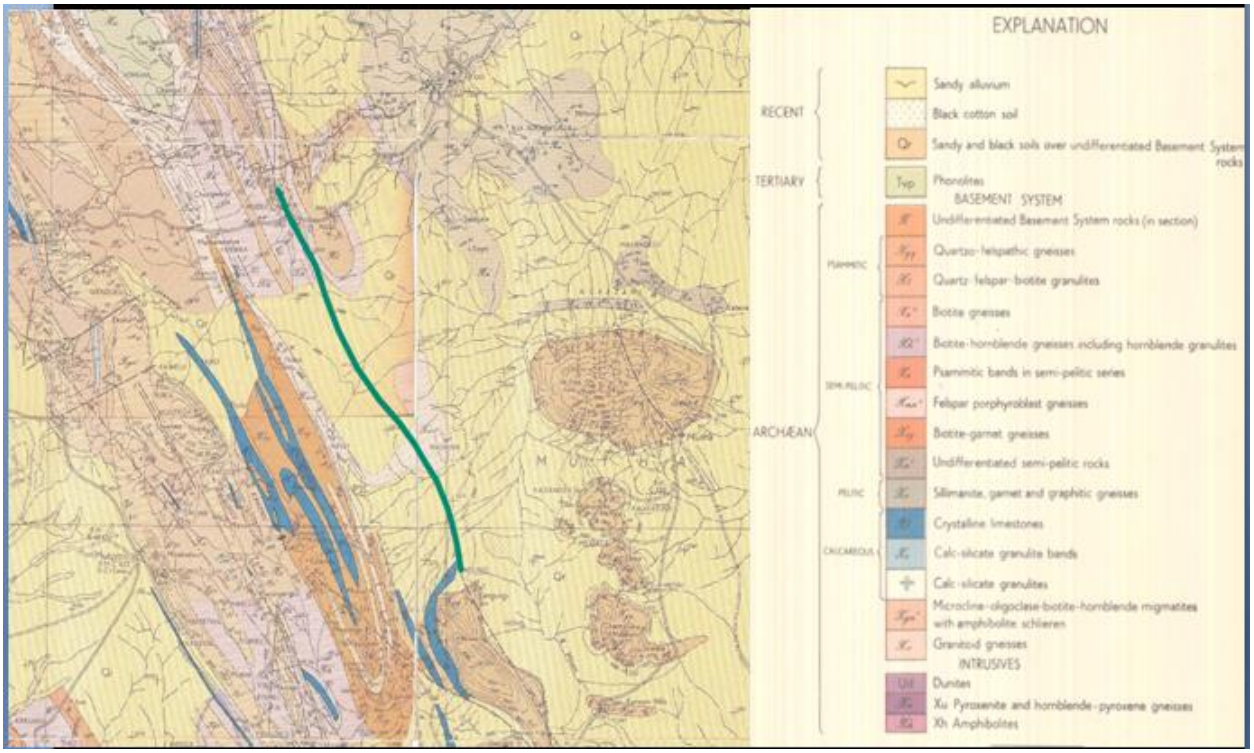

Figure 3: Geological Map of South Kitui (Serggerson, 1957)

The folded syncline structure is clearly shown on the offset diagram of the geological map, most notably is the Ndui and Nzuli as the western limbs of the syncline and the Mathima hill on the Eastern Limb of the syncline . The valley centre is overlain by up to 100 m thick of Quaternary alluvium deposits (yellow).

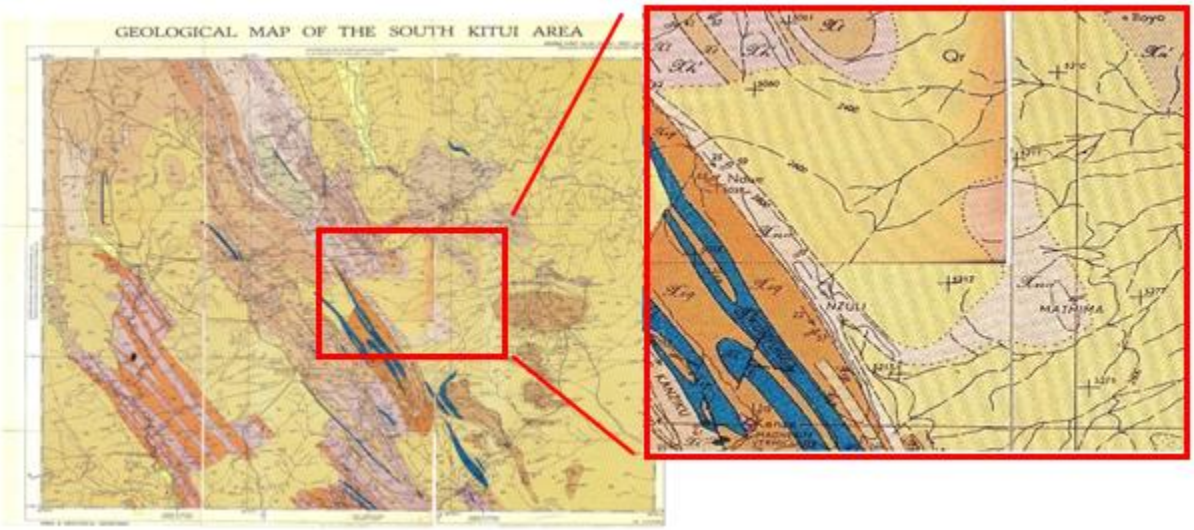

Figure 4: Geological map of the study area

Geophysical techniques were applied to verify the concealed fault zone whose intersection provides for high yielding aquifers and could act as groundwater conduits. The geologically inferred syncline is also intercepted by the inferred faults. This would provide a perfect set up for groundwater.

2.0 Materials and Methods

2.1 Ground Magnetics

Magnetics data was acquired to locate the concealed fractured /faulted basement zones. Susceptibility contrasts on the disintegrated basement was used to map out faults and fractures which may act as groundwater conduits. Geometrics 856 Proton Precession Magnetometer was used to measure total magnetic field to a resolution of 0.1nT. Ground magnetic data was collected perpendicular to the geologically inferred Mutito fault along five straight profiles AA', BB', CC', DD' and EE'. The profiles covered a lateral distance of approximately 4 Km each, running East-West direction across the inferred fault. Each profile had a distance separation of about 1 Km. Magnetic measurements were taken at every 100m meters station along the transect, with the base station readings taken after very one hour, for diurnal corrections.

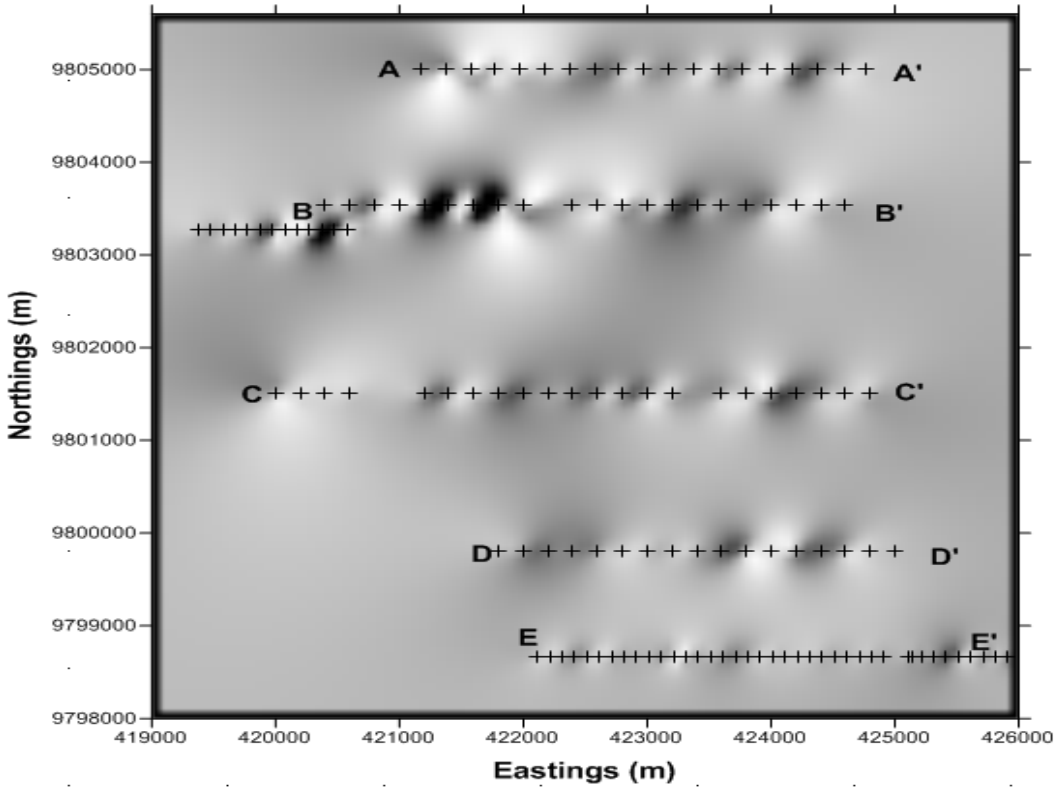

Figure 5: Ground magnetics profiles

3.0 Results and Discussion

After correcting for diurnal variations and geomagnetic field, the filtered magnetic data was uploaded to Surfer 10 software for qualitative analysis. Using the krigging technique, a magnetic Intensity Contour map was plotted. On most profiles, it displayed hachured contours within solid contours, which represent magnetic lows and highs respectively. This continuous magnetic lows within high magnetic anomaly is as a result of local magnetic anomaly of the disintegrated basement rock.

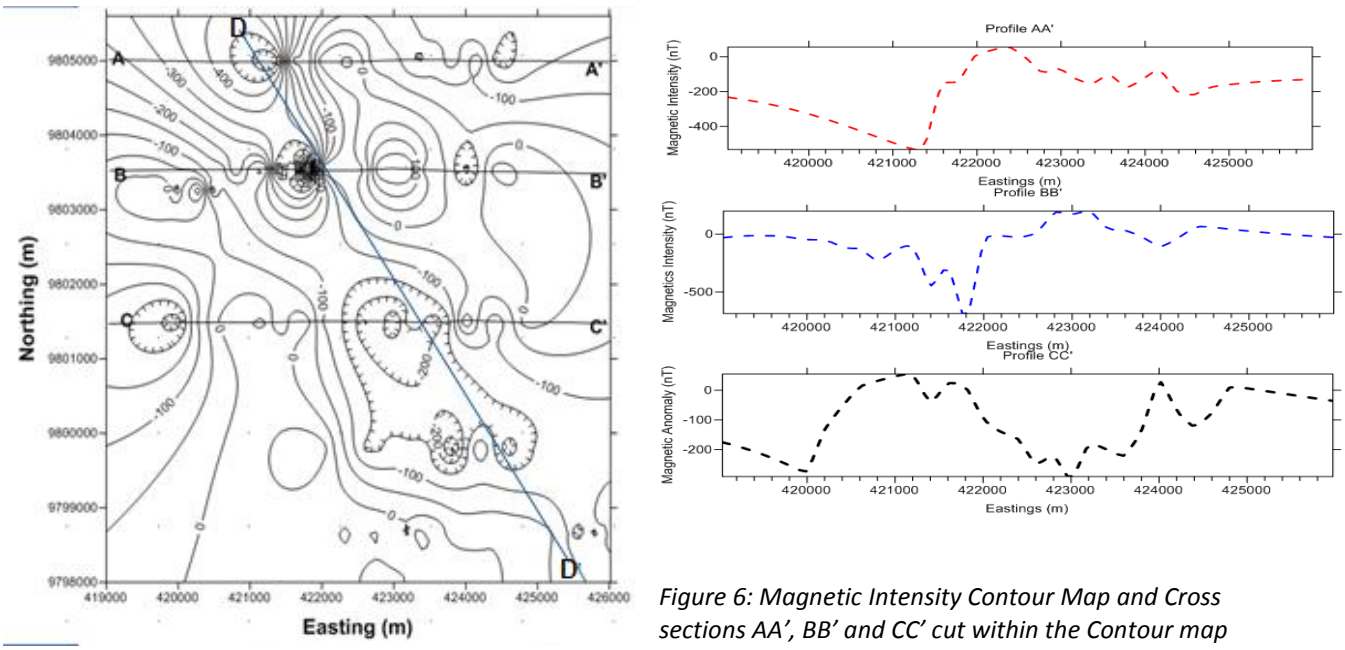

Figure 6: Magnetic Intensity Contour Map and Cross sections AA', BB' and CC' cut within the Contour map

For quantitative analysis, Euler deconvolution was used to create two dimensional (2D) models of discontinuity on the faulted basement. To better constrain the subsurface geology, 0.5 (steep contact) structural index, which is an indication of fault contacts was plotted for all the four profiles.

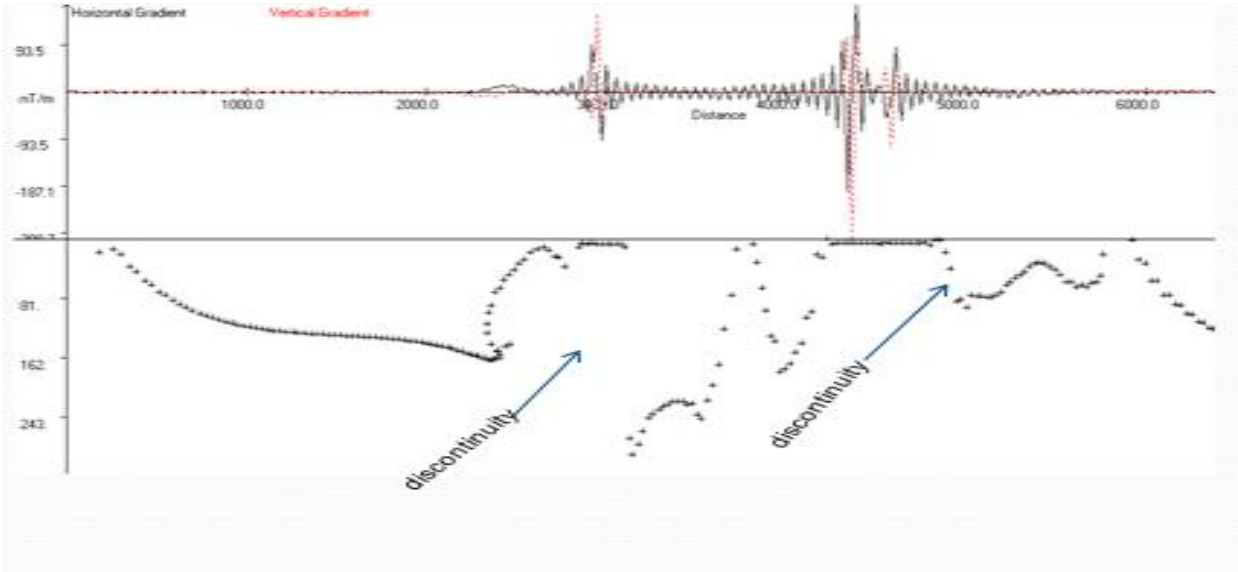

Figure 7: Processed ground magnetic data with 2D Euler solution obtained along traverse AA' with inclination and declination angles of 0.13^o and -24.42^o respectively.Plus (+) signs are Euler solutions for 0.5 structural index

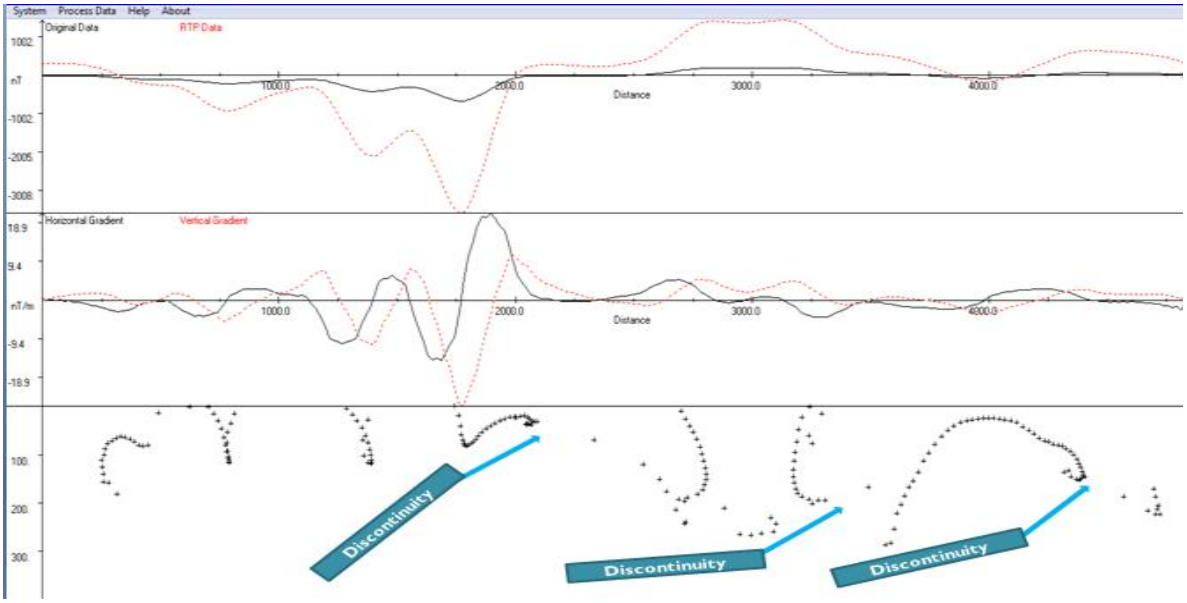

Figure 8: Processed ground magnetic data with 2D Euler solution obtained along traverse BB' with inclination and declination angles of 0.13° and -24.42° respectively.Plus (+) signs are Euler solutions for 0.5 structural index

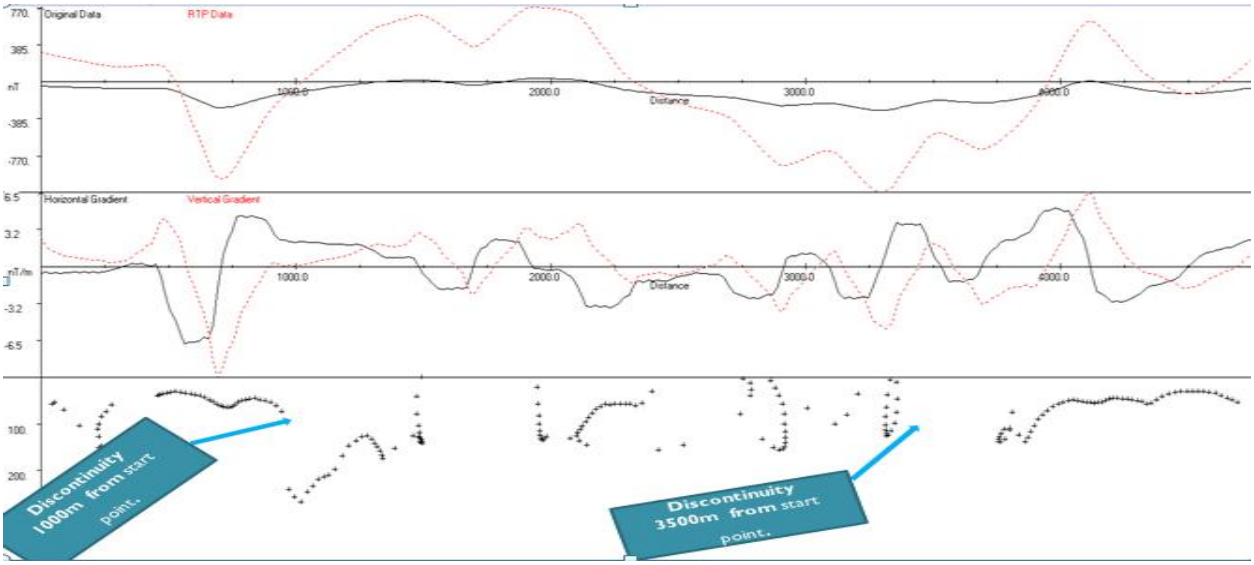

Figure 9: Processed ground magnetic data with 2D Euler solution obtained along traverse CC' with inclination and declination angles of 0.13° and -24.42° respectively.Plus (+) signs are Euler solutions for 0.5 structural index

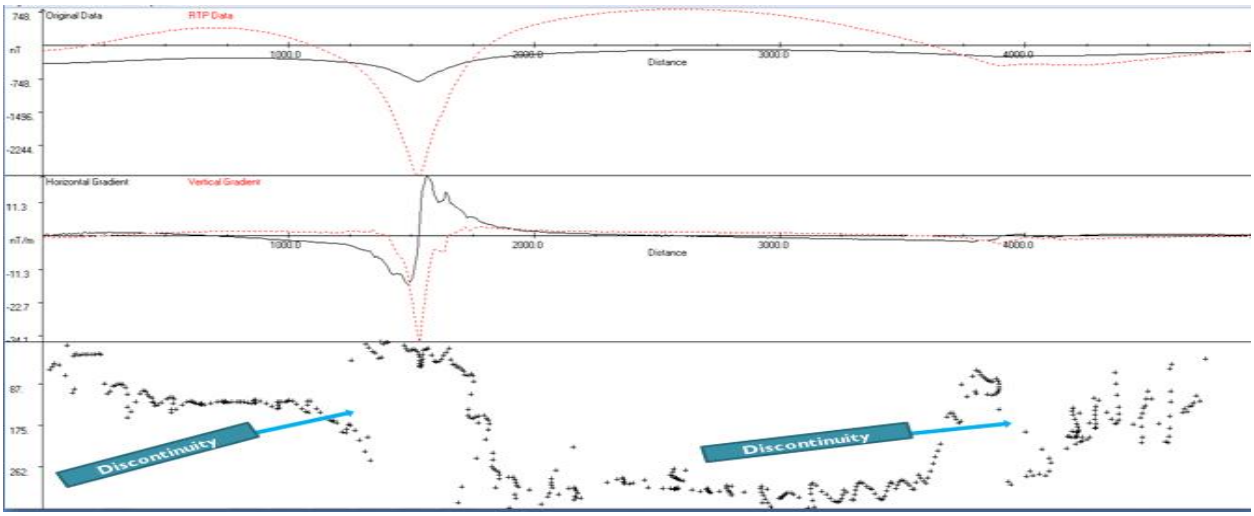

Figure 10: Processed ground magnetic data with 2D Euler solution obtained along traverse DD' with inclination and declination angles of 0.13^o and -24.42^o respectively. Plus (+) signs are Euler solutions for 0.5 structural index

The variations in magnetic amplitudes and the much scattering in the Euler solutions could be attributed to an intense shearing activity and localized anomaly beaneth the profiles, which is also visible in the analytical Contour map.

Transect AA' also has very well defined scattered points that define fault structures along this transect. This undulating signature and the Euler deconvolution solutions clearly show the subsurface faulting/ contacts pattern within this geological unit.
Transect BB' and CC' show a grid of scattered points, signifying a grid of subsurface discontinuity across all the profiles. This is in complete coherence with the structural geological map, by Serggerson (1957), of the Mutito Fault zone, which states that the Mutito Fault may not be a single discontinuity but a grid of about 2 km wide fractures in the geological unit.

Transect DD' is imaged by distinct rifts of the scattered point that signifies a fault structure whose depth is approximately 200meters. A basin structure of 250m depth is also imaged on this same transect, which could imply the geosynclines structure caused by folding, as discussed by Serggerson (1957) in the geological report. From this model also, the fault structure seems to intersect the syncline at an angle.Therefore, from Euler solutions, the Mutito Fault is well defined at depths of about 200m.This is consistently seen in all profiles that were modeled out. These results are in agreement with the magnetic Intensity Contour map that displayed distinct hachured contours within solid contours, which represented distinct magnetic lows within magnetic highs. This continuous discontinuity was seen in each of the three profiles, which had a distance separation of 1 kilometer. This anomaly would most likely signify basement disintegration, which confirms the geological inference of the Mutito Fault.

3.0 Material and Methods

3.1 Electrical Resistivity

Resistivity method was used to map out groundwater potential within the inferred Mutito Fault. Sudden low resistivity values within high resistivity values are the expected signatures for ground water. The resistivity equipment used in this research was a Tigre Geopulse resistivity model, provided by the JKUAT Physics department. In this project, the geo-electrical data was obtained using both the Schlumberger and Wenner arrays. Six Wenner profiles were run perpendicular to the direction of the inferred fault so as to intercept the fault. Profile AA', BB', CC' and EE' had an electrode spacing a=100 meters while Profile BB' and DD' were conducted with an electrode spacing of a=30 meters. This was done to investigate lateral resistivity variation at different depths. Two VES soundings were carried out along profile BB' to determine how resistivity varies with depth.

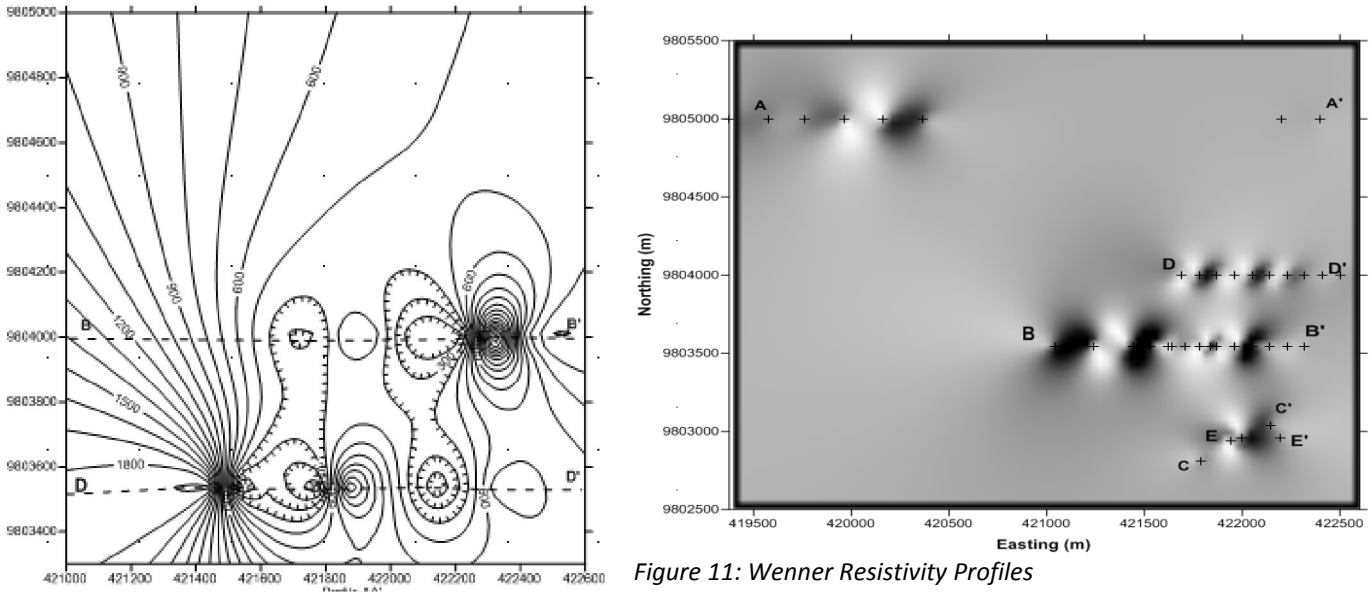

Figure 11: Wenner Resistivity Profiles

4.0 Results and Discussion

For qualitative analysis, the Wenner apparent resistivity data was uploaded in Surfer 10 software. Using the krigging technique, a 2D resistivity anomaly Contour map was plotted. The contour map below shows lateral resistivity anomaly at current depth penetration of a=100 meters.

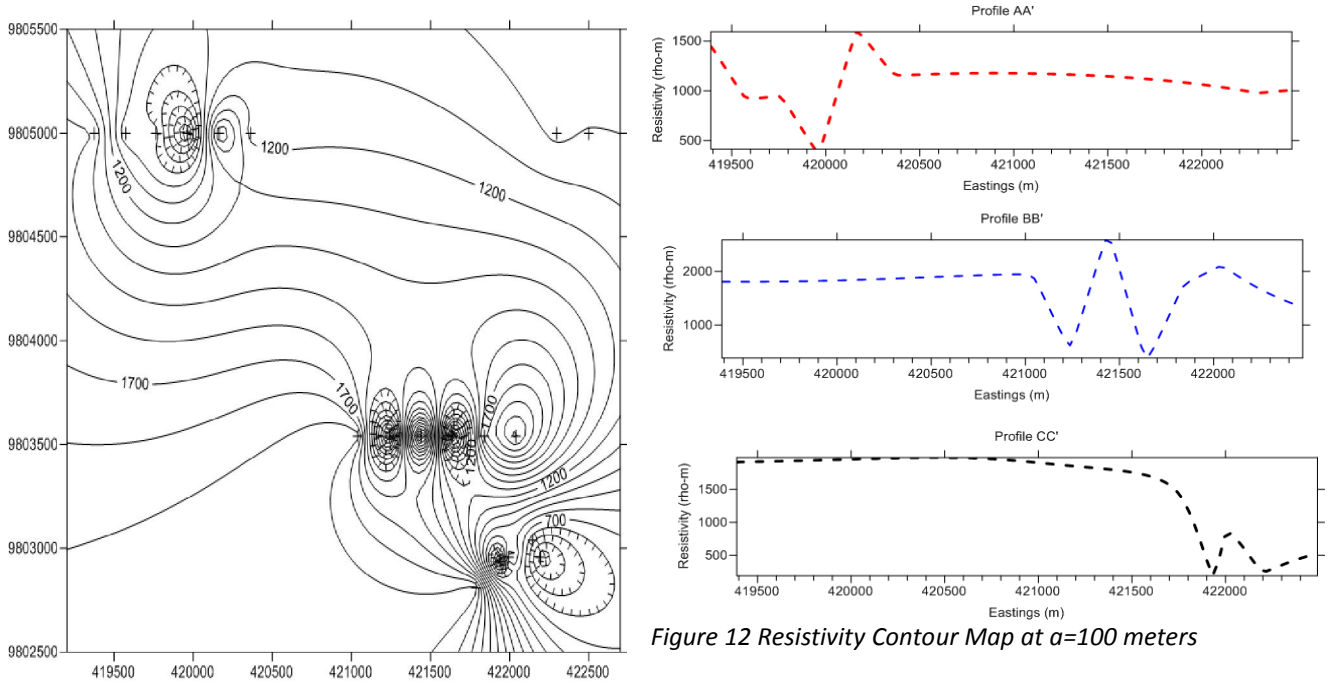

Figure 12 Resistivity Contour Map at a=100 meters

The contour map below shows lateral resistivity anomaly at current depth penetration of a=30 meters

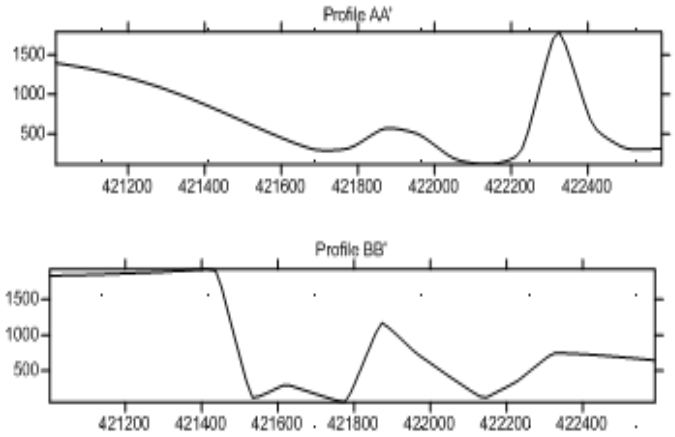

Figure 13: Resistivity Contour Map at a=30 meters

At current depth penetration of 100 m, clear low resistivity anomalies within highly resistivity environment on profiles AA', BB' and CC, would most likely signify groundwater contained within the fault structure in the basement. When a profile with a=30 meters was carried out on profile BB', a similar signature was evident.
Two VES soundings were carried out along profile BB', indicated by two parallel red lines, to determine how resistivity varies with depth.

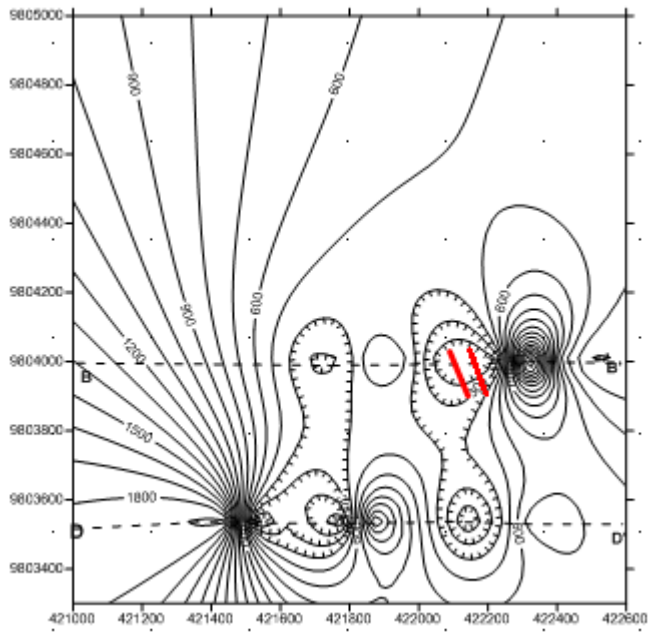

On each transect, two VES stations with a distance separation of 200 meters, were conducted. The two transects were ran parallel to each other at a distance of 150 meters apart. Vertical Electric sounding (VES) logarithmic curves were obtained by plotting the calculated apparent resistivity (ρ) against electrode spacing, AB/2**.**

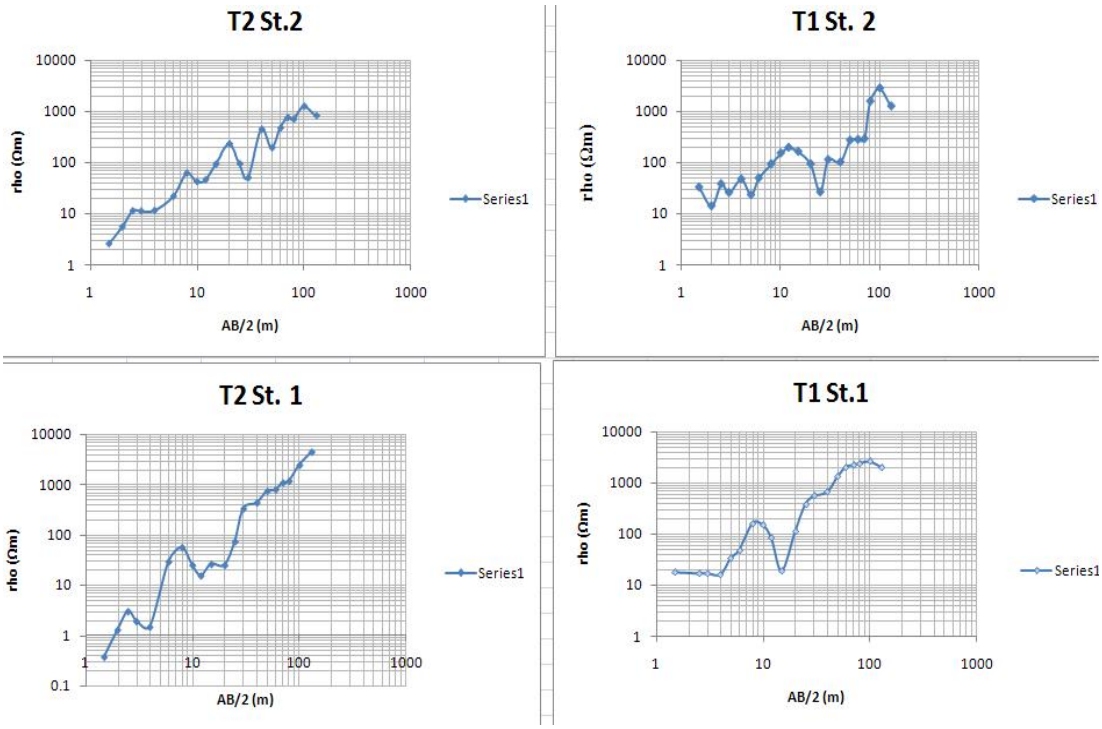

Using IP2WIN software, pseudo section models were produced that show the varying resistivity with depth. The model below show how resistivity varies along the parallel profiles.

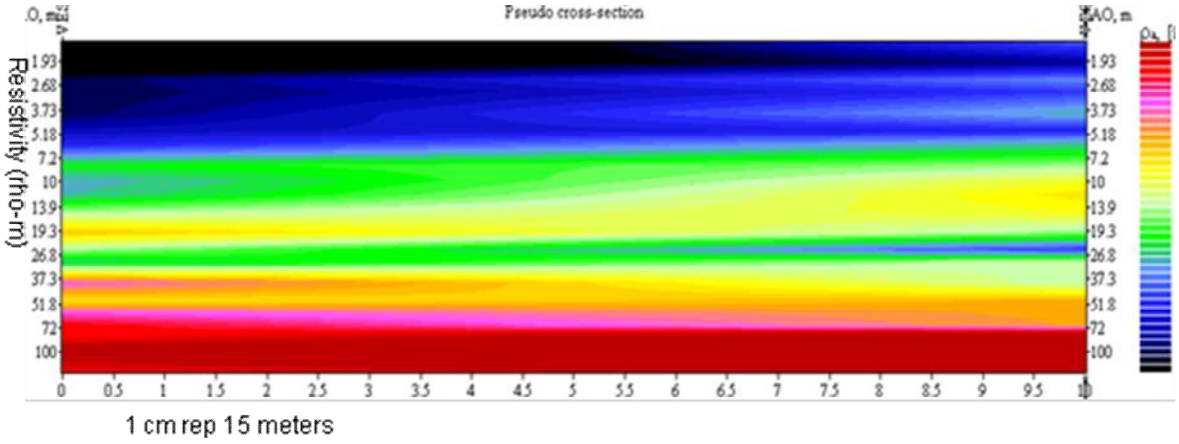

Figure 14: From Right to Left; Transects 2 St. 2 parallel to Transect 1 St. 2

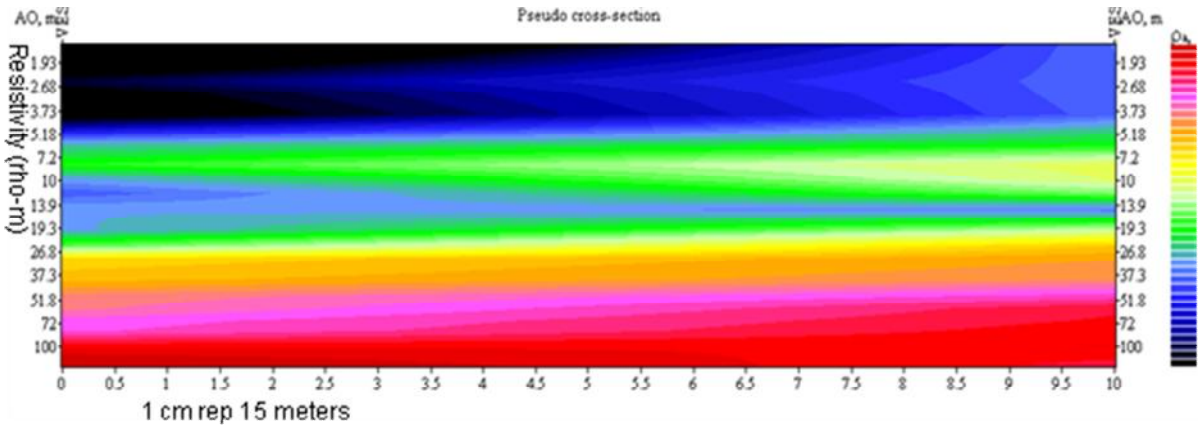

Figure 15 From Right to Left; Transects 2 St. 1 parallel to Transect 1 St. 1

For T1 St.2: There is a similar trend, where the sudden low is seen at depths of AB/2= 12m to about 25m. This would be interpreted as the depth extension of the fault, with low resistivity content (groundwater) at 25m depth from the surface. At depth of AB/2 100m, there also seems to be an apparent shift towards a low anomaly. Since we don't have data past 130m, it is recommended that further studies establish presence of a disrupted trend, which would indicate fracture or aquifer zone at this depth. This trend is also seen in T2. St.2, where the lows occur from a depth of about 20 -30m.

For T1 St.1, there is a sudden drop in resistivity from a depth of AB/2 =10 m to about 15m. This would be interpreted as the depth extension of the fault, with low resistivity content (groundwater) at 15m depth from the surface. At depth of AB/2 100m, there seems to be an apparent shift towards a low anomaly. Since we don't have data past 130m, it is recommended that further studies establish presence of a disrupted trend, which would indicate aquifer zone at this depth. For T2 St.1 , the sudden low is depicted at depths of AB/2 =9m to about 20 m. This transect is parallel to T1. St.1, whose maximum depth is 15m. This would be interpreted as T2. St. 1 being deeper than T1. St.1.

Hence the depth axis can be established by comparing the two parallel transects, which show that the fault is deeping towards the west. When one compares the two parallel transects, T1.St.1 and T2.St. 2, one can tell that the depth axis is towards the west, since the lowest point on T2.St. 2is 30m while that of T1.St. 2 is 25m.

5.0 Conclusion

Comparing previous geological findings and the geophysical results, great coherence in the trend of the inferred fault is evident. According to previous geological report, the fault trends at a 290^{o} bearing, NW-SE direction.

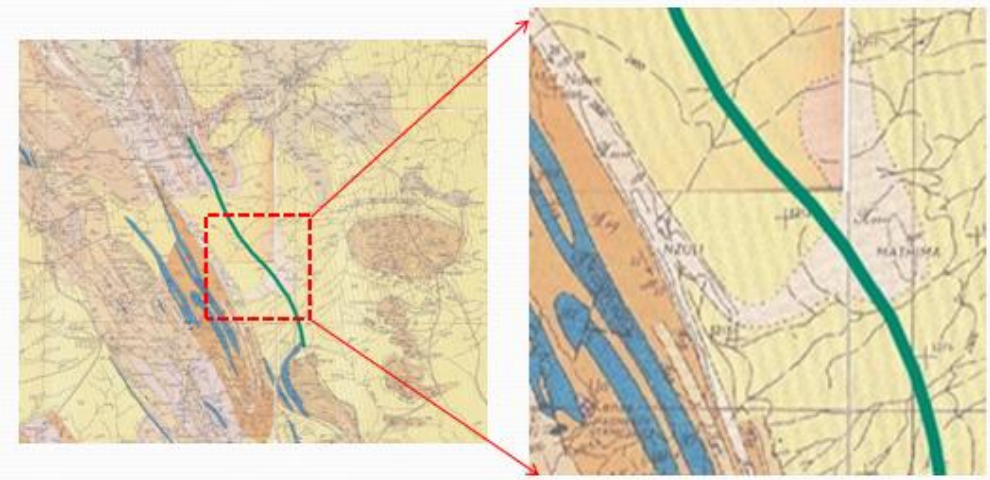

Figure 16: Geological map of South Kitui: Green line shows the geologically inferred Mutito Fault

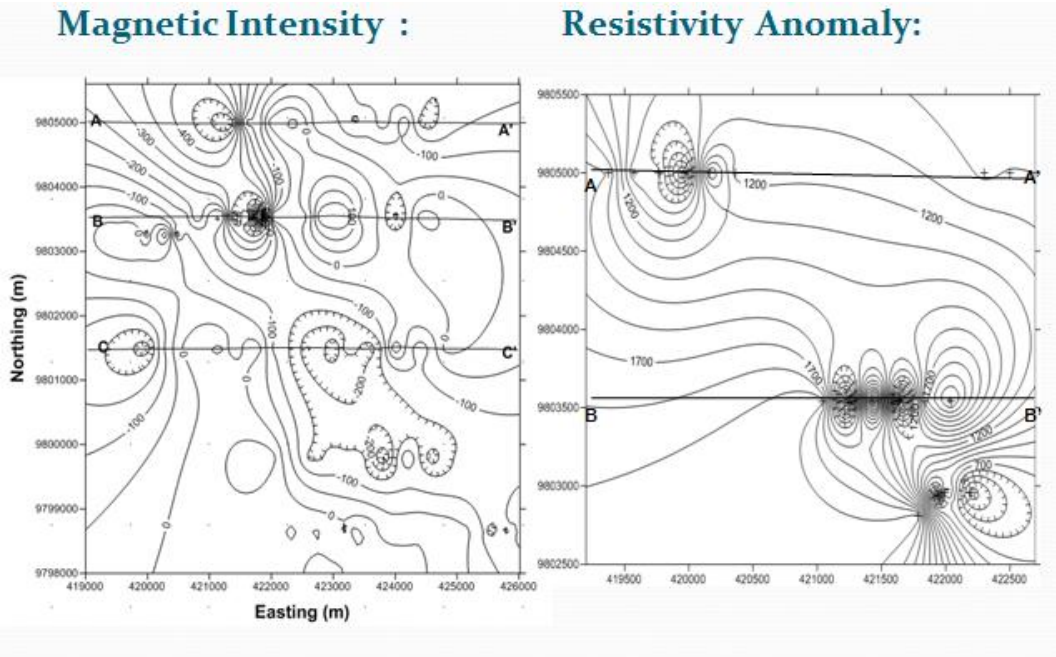

This trend is seen in both magnetic and resistivity, whose anomalies, indicated by the hachured contours, trend in a similar direction, at a similar bearing. These results confirm the presence of the inferred Mutito Fault, which could potentially act as a groundwater conduit in the Kitui hard rock environment.

Since the two methods, magnetic and resistivity were run on similar profiles, it was easy to compare the two data sets so as to see any correlation. A few Cross sections along similar profiles, within the Magnetic Intensity Contour map and the resistivity Contour map, were cut so as to investigate coherence.

Comparing Profile AA' for both Magnetics and Resistivity

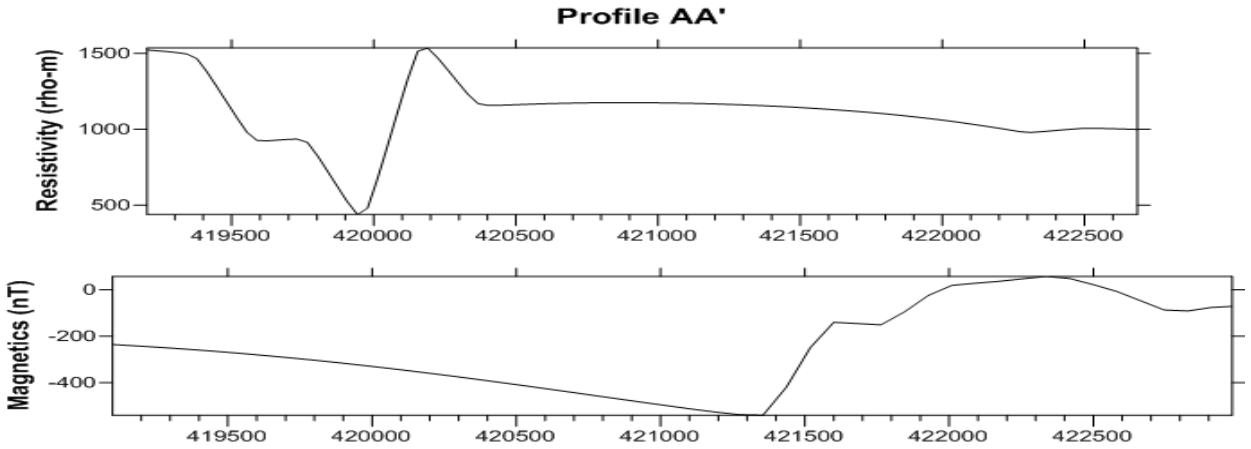

The Magnetic Intensity cross section AA', run on Northing 9805000 clearly show distinct high and low magnetic responses. Between Easting 421500 and 422000, a steep gradient that signify the position of the subsurface fault is evident. The Resistivity cross section AA' also displays very distinct low resistivity measurements which signify groundwater, at points close to the magnetic anomaly. This can therefore be interpreted as low resistivity groundwater, flowing in the fault structure.

Comparing Profile AA' for both Magnetics and Resistivity

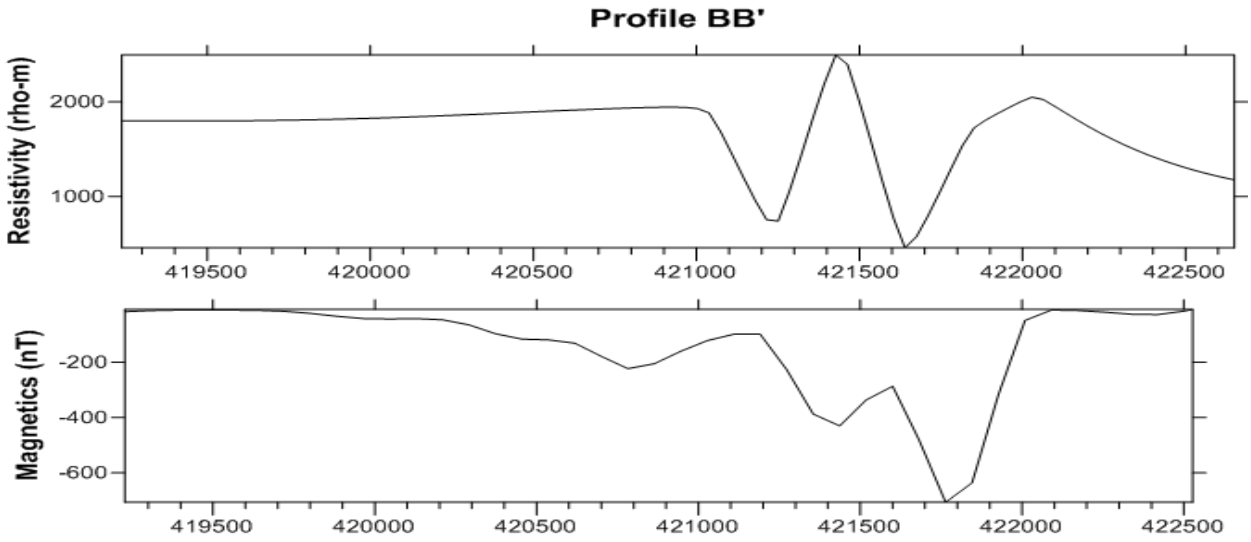

The Magnetic Intensity cross section BB', cut on Northing 9803500 clearly show similar distinct high and low magnetic responses. This profile is 1.5 Km away from the previous profile AA'. Between Easting 421400 and 422000, a steep gradient that signify the position of the subsurface fault is evident. The Resistiviy cross section BB' also displays very distinct low resistivity measurements which signify groundwater, at the same point, Easting 421400 and 422000. This can therefore be interpreted as low resistivity groundwater, flowing in the fault structure.

Therefore, from the analysis of the two geophysical techniques, the locations with the similar correlations of the two data sets are indicated in the topographical map below. The best location however, with the best correlation is point 9803500 Northing 421700 Easting. This would be the area with the highest chance of groundwater drilling success.

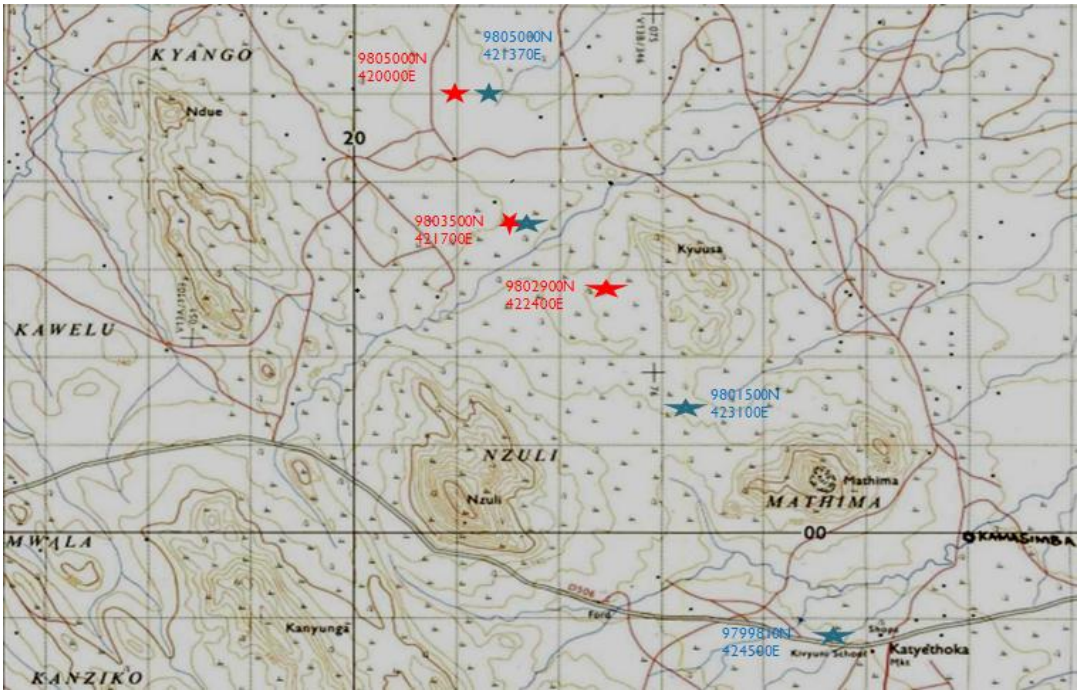

Figure 17: Topographical Map of South Kitui area: Red star indicates location of distinct low resistivity while blue star indicates location of distinct magnetic lows

Acknowledgement

I first want to acknowledge God for the strength to carry out this project. Secondly, the two main supervisors, Dr. Maurice O.K and Dr. John Githiri, whose guidance was key in making sure that the data acquisition and analysis was up to standard. This project would not have succeeded without the generous funding from Society and Exploration Geophysicist (SEG) which provided the funds necessary to undertake this project. Dr. Cezar I. and Jefferey S., the SEG representatives, also brought an international aspect to this project as they shared their geophysical expertise in this project. I also want to acknowledge the JKUAT students, among them Elly Bogi and Hillary Korir, who greatly helped in acquiring and analyzing the data. Lastly, many thanks to JKUAT Physics department that availed all the instruments for this project.

References

Barker, R.D. (2001). “Imaging fractures in hard rock terrain”.

http://www.bham.ac.uk/EarthSciences/researchUniversity of Birmingham, UK

Hasbrouck, J. and Morgan, T. (2003). *Deep water exploration using Geophysics*, Hasbrouck Geophysics Inc. and Layne Christensen Company, Southwest Hydrology conference, Texas.

Keys S. W. and MacCary M.L. (1971). *Application of Borehole Geophysics to Water Resource investigation,* United States Geological Survey, Washington.

Nyamai, C. M., Mathu, E. M., Opiyo-Akech. N. and Wallbrecher. E. (2003). A Reappraaisal of the Geology, Geochemistry,Structures and Tectonics of the Mozambique belt in Kenya, East of the Rift System, *African Journal of Science and Technology (AJST),***4**: pp. 51-71.

Patangay. N. S. and Murali, S. (1998*). Principles and Applications of Groundwater Geophysics*, Association of Exploration Geophysicists, India.

Saggerson, E.P. (1957). Geology of South Kitui area, *Rept. Geological Surv*. *Kenya*, **1**: pp. 37.

Sharma, S. P. and Baranwal, V. C. (2005). Delineation of groundwater-bearing fracture zones in a hard rock area integrating Very Low Frequency Electromagnetic and Resistivity data, *Journal of Applied Geophysics,* **57**: pp. 155-166.